The juvenile myoclonic epilepsy-related protein EFHC1 interacts with the redox-sensitive TRPM2 channel linked to cell death

Masahiro Katano[1], Tomohiro Numata[1], Kripamoy Aguan[2], Yuji Hara[1], Shigeki Kiyonaka[1], Shinichiro Yamamoto[1], Takafumi Miki[1], Seishiro Sawamura[1], Toshimitsu Suzuki[2], Kazuhiro Yamakawa[2]& Yasuo Mori[1,3]

[1]Laboratory of Molecular Biology, Department of Synthetic Chemistry and Biological Chemistry, Graduate School of Engineering, and Laboratory of Environmental Systems Biology, Department of Technology and Ecology, Hall of Global Environmental Studies, Kyoto University, Kyoto 615-8510, Japan

[2]RIKEN Brain Science Institute, Wako-shi, Saitama 351-0198, Japan

[3]CREST, JST, Chiyoda-ku, Tokyo 102-0075, Japan

Correspondence and requests for materials should be addressed to Y.M.

(e-mail: mori@sbchem.kyoto-u.ac.jp)

Abstract

The transient receptor potential M2 channel (TRPM2) is the Ca^{2+}-permeable cation channel controlled by cellular redox status via β-NAD^{+} and ADP-ribose (ADPR). TRPM2 activity has been reported to underlie susceptibility to cell death and biological processes such as inflammatory cell migration and insulin secretion. However, little is known about the intracellular mechanisms that regulate oxidative stress-induced cell death via TRPM2. We report here a molecular and functional interaction between the TRPM2 channel and EF-hand motif-containing protein EFHC1, whose mutation causes juvenile myoclonic epilepsy (JME) via mechanisms including neuronal apoptosis. *In situ* hybridization analysis demonstrates TRPM2 and EFHC1 are coexpressed in hippocampal neurons and ventricle cells, while immunoprecipitation analysis demonstrates physical interaction of the N- and C-terminal cytoplasmic regions of TRPM2 with the EFHC1 protein. Coexpression of EFHC1 significantly potentiates hydrogen peroxide (H_2O_2)- and ADPR-induced Ca^{2+} responses and cationic currents via recombinant TRPM2 in HEK293 cells. Furthermore, EFHC1 enhances TRPM2-conferred susceptibility of HEK293 cells to H_2O_2-induced cell death, which is reversed by JME mutations. These results reveal a positive regulatory action of EFHC1 on TRPM2 activity, suggesting that TRPM2 contributes to the expression of JME phenotypes by mediating disruptive effects of JME mutations of EFHC1 on biological processes including cell death.

1. Introduction

Mammalian homologues of *Drosophila* transient receptor potential (TRP) protein form cation channels activated by sensing a variety of physical and chemical stimuli [1,2]. TRPM2 is a Ca^{2+}-permeable channel activated by ADP-ribose (ADPR) [3,4] and oxidative stress via β-NAD^{+}[5] and/or ADP-ribose [6–8], and regulated by various factors [9–11]. TRPM2 activity has been reported to underlie biological processes such as cell death [5], inflammatory cell migration [8], and insulin secretion [12].

Juvenile myoclonic epilepsy (JME) is the most common form of idiopathic generalized epilepsy, accounting for 10–30% of all epilepsies [13]. The gene encoding EF-hand motif-containing protein, EFHC1, has been identified in the region on chromosome 6p12-p11 associated with JME [14]. EFHC1 is reported to be expressed in brain neurons [14,15], and in ependymal cells of ventricle walls and other cells that possess motile cilia and flagella [16–18]. In neuronal cells, EFHC1 increases voltage-dependent R-type Ca^{2+} channel ($Ca_V2.3$) currents and induces neuronal death. However, the previous report [14] suggests that the EFHC1-dependent $Ca_V2.3$ Ca^{2+} current increase is not an exclusive mechanism that underlies EFHC1-induced neuronal death reversed by the JME mutations. EFHC1 may interact with an additional number of proteins in cell death sensitive to JME mutations. With regard to Ca^{2+} channels linked to cell death, TRPM2 has been reported to elicit hydrogen peroxide (H_2O_2)- and tumor necrosis factor α-induced cell death [5,19]. Interestingly, reactive oxygen species (ROS) are reported to be constitutively produced in rat hippocampus [20]. The idea that TRPM2 can be the missing protein linking cell death to EFHC1/JME prompted us to test interaction between EFHC1 and TRPM2. Furthermore, it is important to note that genetic disruption of EFHC1 causes enlargement of ventricles and reduced

ciliary beating frequency of ependymal cilia in ventricle [21], and that EFHC1 interacts with microtubules to regulate cell division and cortical development [22]. These recent reports also provide important bases to consider possibilities other than the original scenario focusing on the major role of cell death via R-type Ca^{2+} channels in the expression of JME phenotypes.

We show here physical association between EFHC1 and TRPM2. EFHC1 enhanced the H_2O_2 sensitivity of TRPM2 channel activation and cell death. The obtained results may suggest that EFHC1 regulates voltage-independent TRPM2 Ca^{2+} channels to control Ca^{2+} homeostasis in neuronal death.

2. Experimental procedures

2.1. Cell Culture and Recombinant Expression in HEK293 Cells

The expression plasmid for human TRPM2 (hTRPM2) was constructed as described previously [5]. HEK293 (ATCC) cells were cultured in Dulbecco's modified Eagle's medium (DMEM) containing 10% fetal bovine serum (FBS), 30 units/ml penicillin, and 30 μg/ml streptomycin. HEK293 cells were co-transfected with pEGFP-EFHC1 or pEGFP-C2 vector and one of pCI-neo-hTRPM2 and the vector pCI-neo. Transfection was carried out using SuperFect Transfection Reagent (QIAGEN). Cells were trypsinized and diluted with DMEM and plated onto glass coverslips 24 h after transfection. Then cells were subjected to measurements 6–24 h after plating on the coverslips. TRPM2-expressing cells were selected through detection of GFP.

2.2. Immunofluorescence Staining

After 24 h of transfection with pcDNA4mycHisA-hTRPM2 and pEGFP-EFHC1 using SuperFect, HEK293 cells were plated onto poly-L-lysine coated glass base dishes (IWAKI, Chiba, Japan). Cells were fixed with 4% paraformaldehyde (PFA), and then permeabilized with 0.1% Triton X-100. The cells were incubated with primary antibody, anti-myc antibody (Invitrogen), followed by subsequent incubation with the Cy3-conjugated anti-mouse secondary antibody. The fluorescence immunoimages were acquired with a confocal laser-scanning microscope (Fluoview 500; Olympus, Tokyo, Japan) equipped with krypton/argon and helium/neon ion lasers. The emitted fluorescence was collected through an objective lens with a 40 times magnification for HEK293 cells.

2.3. In Situ Hybridization Histochemistry

For histological staining of the central nervous system (CNS), 8-week-old mice (C57BL/6) were deeply anesthetized with an overdose of Nembutal and then transcardially perfused by 0.9% NaCl, followed by 4% PFA in 0.1 M phosphate buffer (pH 7.4). The brains of the animals were dissected. Cryoprotection of the tissue blocks in 40% sucrose for 24 h at 4°C was followed by histological sectioning on a cryostat (Leica). For details about *in situ* hybridization histochemistry, see Kagawa et al. [23]. Briefly, in vitro transcribed DIG-labeled cRNA probe was generated against template EFHC1 cDNA fragment (319–1376) of mouse EFHC1 using DIG RNA labeling kit (Roche Applied Science). The probe (0.1 μg/ml) was hybridized overnight to mouse CNS histological 35-μm-thick sections at 50°C. Positive signals were detected by alkaline phosphatase-conjugated anti-digoxigenin antibody and the nitro blue

tetrazolium/5-bromo-4-chloro-3’-indolyl phosphate reaction.

2.4. Co-immunoprecipitation of TRPM2 and EFHC1 Proteins

Physical interaction between recombinant TRPM2 and EFHC1 was detected by co-immunoprecipitational analysis as previously described [14,24]. Briefly, FLAG-tagged $Ca_V2.3$ C-terminus, TRPM2 N-terminus (amino acid residues 1–738), TRPM2 C-terminus (1057–1503), full-length TRPM2, endophilin or EFHC1 was coexpressed with myc-tagged EFHC1 or GFP-tagged EFHC1 in HEK293 cells, and cell lysates were immunoprecipitated by antibody to FLAG (Sigma). $Ca_V2.3$ C-terminus and endophilin were used as a positive and a negative control for EFHC1, respectively [14]. Blots were incubated with anti-myc antibody (Santa Cruz Biotechnology) or anti-GFP antibody (Clontech), and stained using Western Lightning Chemiluminescence Reagent Plus (Perkin Elmer Life Sciences).

For characterization of physical interaction between native TRPM2 and EFHC1, mouse brain microsomes were prepared as described previously [24]. Proteins were extracted from the microsomes with RIPA buffer (pH 8.0) containing 0.1% SDS, 0.5% sodium deoxycholate, 1% Nonidet P-40, 150 mM NaCl, 50 mM Tris-HCl, 1 mM PMSF, and 10 μg/ml leupeptin, then centrifuged at 17,400 × g for 30 min to remove cell debris. For coimmunoprecipitation, the cell lysate was incubated with anti-TRPM2 antibody [8] for 2h. Then, the immunocomplexes were incubated with protein A-agarose beads (Santa Cruz) for 1h, and the beads were washed with RIPA buffer. Immunoprecipitated proteins were separated by 10% SDS-PAGE and electrotransferred onto a PVDF membrane. The blots were incubated with anti-EFHC1 monoclonal antibody [17], and visualized using the ECL system (Thermo Scientific).

2.5. In vitro Protein Interaction Studies

We produced the respective proteins of DNA constructs (FLAG-TRPM2 N-terminus, FLAG-TRPM2 C-terminus, FLAG-endophilin and myc-EFHC1) in rabbit reticulolysate by *in vitro* transcription and translation using Quick Coupled TNT Systems (Promega). We used 3 μg of each plasmid DNA in 50 μl of rabbit reticulolysate for translation and incubated for 2 h at 30°C. We then added 50 μl of translated myc-EFHC1 rabbit reticulolysate to each of the 50 μl rabbit reticulolysate containing translated FLAG-tagged proteins and made the volume up to 500 μl with buffer containing 150 mM NaCl, 0.1% Triton X-100 and 50 mM Tris-HCl (pH 7.5). We incubated the mixture for 4 h at 40°C, added anti-myc antibody conjugated to agarose beads (Nacalai Tesque, Kyoto, Japan) and further incubated for 2 h. The beads were washed six times with same buffer and the bound proteins were eluted by adding 40 μl of 2×sample buffer followed by boiling for 3 min. The eluted samples were run on 4/20% SDS-PAGE and transferred to nitrocellulose membrane. The membrane was immuno-probed with anti-FLAG antibody conjugated to HRP and stained with ECL-Plus kit (GE healthcare). Following the first development, the membrane was stripped with Re-Blot Plus buffer (Millipore) and re-immunoprobed with anti-myc antibody.

2.6. Intracellular Ca^{2+} Concentration ($[Ca^{2+}]_i$) Measurements

HEK293 cells on coverslips were loaded with fura-2 by incubation in DMEM containing 1 μM fura-2/AM (Dojindo, Kumamoto, Japan) and 10% FBS at 37°C for 40 min. The coverslips were then plated in a perfusion chamber mounted on the stage of the microscope. Fluorescence images of the cells were recorded and analyzed with a

video images analysis system (ARGUS-20/CA; Hamamatsu Photonics, Shizuoka, Japan). The fura-2 fluorescence at an emission wavelength of 510 nm (bandwidth, 20 nm) was obtained at room temperature by exciting fura-2 alternately at 340 and 380 nm (bandwidth, 11 nm). The 340:380 nm ratio images were obtained on a pixel-by-pixel basis. H_2O_2 was diluted to their final concentrations in HEPES-buffered saline (HBS) containing 107 mM NaCl, 6 mM KCl, 1.2 mM $MgSO_4$, 2 mM $CaCl_2$, 11.5 mM glucose, 20 mM HEPES, adjusted to pH 7.4 with NaOH, and applied to the cells by perfusion.

2.7. Electrophysiology

Whole-cell currents were recorded at room temperature using the conventional whole-cell configuration [25]. Pipette resistance ranged from 2 to 4 MΩ when filled with the pipette solution described below. The pipette solution was: 1.3 mM $CaCl_2$, 40 mM CsCl, 105 mM CsOH, 2 mM $MgCl_2$, 5 mM EGTA, 2 mM ATP Na_2, 105 mM aspartate, 5 mM HEPES, adjusted to pH 7.2 with CsOH (50 nM calculated free Ca^{2+}). The '2 mM Ca^{2+}-NaCl solution' contained : 125 mM NaCl, 1.2 mM $MgCl_2$, 2 mM $CaCl_2$, 10 mM glucose, 11.5 mM HEPES, 51 mM mannitol, adjusted to pH 7.4 with NaOH. For Supplementary Fig. 2, 5 mM EGTA was replaced with 5 mM BAPTA. The free Ca^{2+} concentration was from 1 nM to 100 μM calculated with CaBuf software (provided by Dr. Droogmans, G., Katholieke Universiteit Leuven, Leuven, Belgium). $[Ca^{2+}]_i$ concentration-response plots were fitted to the logistic equation: $I = (A_{max}-A_0)/[1+(X/EC_{50})^n]+A_0$, where I is the normalized current amplitude, X is the $[Ca^{2+}]_i$ concentration; n is Hill coefficient; EC_{50} is the concentration of $[Ca^{2+}]_i$ that generate 50% of maximal current.

2.8. Assays for Cell Death

Cell death was induced by H_2O_2 in HEK293 cells 36 h after transfection. After cells were exposed to various concentrations of H_2O_2 for 20 min, cell death was assessed by counting cells which failed to show trypan blue exclusion after a 5-min incubation with 0.4% trypan blue diluted by HBS solution containing 2 mM Ca^{2+} at room temperature [5].

2.9. Statistical analyses

All data are expressed as means ± S.E.. We accumulated the data for each condition from at least three independent experiments. The statistical analyses were performed using the Student's *t*-test. *P* values < 0.05 were considered significant.

3. Results

3.1. EFHC1 Physically Associates with TRPM2

To assess the localization of TRPM2 and EFHC1 in brain tissues, *in situ* hybridization analysis was performed. TRPM2 was expressed in hippocampal pyramidal neurons [5,26,27] and ependymal cells in ventricle walls, where EFHC1 was coexpressed as previously reported (Fig. 1A). The result suggests that TRPM2 and EFHC1 are co-localized in the same cells in the brain. We next examined whether EFHC1 and TRPM2 coexpressed in the same cells are physically associated. Extracts prepared from HEK293 cells transiently expressing EFHC1 plus full-length TRPM2 and from mouse brain microsomes were subjected to co-immunoprecipitation experiments (Fig. 1B and 1C). The obtained data suggest protein-protein interaction between TRPM2 and EFHC1.

To identify the interaction site of TRPM2 with EFHC1, extracts prepared from HEK293 cells transiently expressing EFHC1 plus TRPM2 N- or C-terminus were subjected to co-immunoprecipitation experiments. Myc-EFHC1 was co-immunoprecipitated with $Ca_V2.3$ C-terminus, and TRPM2 N- and C-terminus but not with endophilin [14] (Fig. 1D). The specificity of the interaction between TRPM2 N- or C-terminus and EFHC1 was also tested using *in vitro* translated proteins. Myc-tagged EFHC1 brought down FLAG-tagged TRPM2 N- or C-terminus, but not endophillin (Fig 1E). These results suggest the physical association of EFHC1 with TRPM2 via its putatively cytoplasmic TRPM2 N- and C-terminus. This association is supported by co-immunostaining of TRPM2 and EFHC1 proteins in HEK293 cells. As demonstrated in Fig. 1F, confocal images reveal the subcellular site such as the plasma-membrane area shared by TRPM2 and GFP-EFHC1.

3.2. EFHC1 Potentiates TRPM2 Channel Activity in HEK293 Cells

To elucidate the functional impacts of the physical interaction between the EFHC1 and the TRPM2 channel, we examined the effects of EFHC1 on rises of $[Ca^{2+}]_i$ mediated by TRPM2 expressed in HEK293 cells. Since we have previously shown that the TRPM2 channel is activated by H_2O_2 which induces oxidative stress [5], the effects of coexpression of EFHC1 on H_2O_2-induced $[Ca^{2+}]_i$ rises via TRPM2 were tested. EFHC1 coexpression significantly potentiated TRPM2-mediated $[Ca^{2+}]_i$ rises in response to 30–100 μM H_2O_2, and shifted the dose response relationships to a lower concentration (Fig. 2A and B). Maximal response of TRPM2 to H_2O_2 (1 mM) was unaffected by EFHC1 coexpression (Fig. 2B). Importantly, EFHC1 failed to potentiate Ca^{2+} release from intracellular Ca^{2+} stores and Ca^{2+} influx induced by 100 μM ATP stimulation of

the endogenous purinergic receptors in HEK293 cells (Supplementary Fig. 1) [1,25,28]. These results explicitly suggest a functional significance of association between EFHC1 and TRPM2 that positively regulates the activity of TRPM2 channels.

The effect of EFHC1 on ionic currents mediated by TRPM2 induced by ADPR was also examined using a whole-cell mode of patch clamp recording at a holding potential of –60 mV in TRPM2-expressing cells. TRPM2 current was induced by its activation trigger ADPR [3,4]. In cells expressing EFHC1 and TRPM2, significant inward currents were evoked by ADPR at a concentration of 100 μM (3.48 ± 0.09 nA), while it induced only-marginal inward currents in cells expressing TRPM2 alone (0.56 ± 0.09 nA, $P<0.05$) (Fig. 2C–E). Since important biological roles played by EF-hand proteins include regulation of trafficking of associating channel molecules to the plasma membrane [29,30], we examined whether EFHC1 protein affects the subcellular distribution of TRPM2 in response to H_2O_2 using a microscope. The distribution of GFP-TRPM2 fusion protein transfected alone or co-transfected with EFHC1 was not significantly altered by the application of 100 μM H_2O_2 in HEK293 cells (data not shown). Considering the major involvement of ADPR in activation TRPM2 channels by H_2O_2 [6], these data are consistent with the idea that EFHC1 potentiates ADPR sensitivity to enhance H_2O_2 sensitivity in TRPM2 channels.

Inasmuch as TRPM2 carries the EF-hand motif, EFHC1 can be involved in Ca^{2+} sensitivity of TRPM2 channel [3,5,27,31]. To examine this possibility, ADPR-induced whole cell currents in TRPM2-expressing HEK293 cells transfected with EFHC1 were measured at various $[Ca^{2+}]_i$. TRPM2 currents of GFP- or GFP-EFHC1-coexpressing cells were respectively dose dependent with a EC_{50} value of 117 ± 35 or 155 ± 70 μM (Supplementary Fig. 2A). Extracts prepared from HEK293 cells transiently expressing

EFHC1 plus TRPM2 were subjected to co-immunoprecipitation experiments in the presence of Ca^{2+}. Addition of Ca^{2+} failed to affect interaction between TRPM2 and EFHC1 (Supplementary Fig. 2B). Thus, it is unlikely that EFHC1 is involved in regulation of Ca^{2+} sensitivity of TRPM2 channel activation or is influenced by Ca^{2+} in TRPM2 interaction.

3.3. EFHC1 Facilitates TRPM2-Dependent Cell Death in Response to H_2O_2

Many reports have indicated that excessive production of ROS is related to neurodegenerative diseases such as Parkinson's disease or amyotrophic lateral sclerosis [32], while ROS also mediate normal cellular functions [33]. We have previously revealed an important involvement of TRPM2 channels in redox-induced cell death of insulinoma and monocytic cell-lines [5]. The effects of coexpression of EFHC1 protein on H_2O_2 induced-cell death in TRPM2-expressing HEK293 cells were examined using trypan blue exclusion assay. As shown in Fig. 3, the percentages of dead cells induced by treatment with 30, 100, and 300 μM H_2O_2 among TRPM2-expressing cells were increased by EFHC1 coexpression (Fig. 3). Cell death trigged by H_2O_2 at these concentrations was abolished in the presence of the anti-oxidant glutathione (1 mM) (data not shown). Thus, EFHC1 enhances cell death mediated by TRPM2 channels.

3.4. JME mutations alter the effects of EFHC1 on TRPM2 channel function

In the previous study, we revealed reversing effects of mutations associated with JME on EFHC1 function [14]. However, the cell-death effect of EFHC1 on cultured neurons differed from the enhancing effect of EFHC1 on $Ca_V2.3$ Ca^{2+} currents in susceptibility to suppression by JME mutations: some of the mutations, which nearly abolished the

cell-death effect, only weakly suppressed the enhancing effect. Therefore, in reducing EFHC1-mediated neuronal cell death, JME mutations may reverse EFHC1 effects on Ca^{2+} signaling-regulating molecules other than $Ca_V2.3$. Fig. 4A demonstrates a significant reversal of EFHC1-mediated enhancement of H_2O_2-induced TRPM2 activity by JME mutations (P77T, D210N, R221H, F229L, and D253Y), but not by coding polymorphisms (R159W, R182H and I619L) that were also present in the control population [14]. Potentiation of ADPR-activated TRPM2 currents was also reversed by the JME mutations but not by coding polymorphisms (Fig. 4B). EFHC1-induced potentiation of TRPM2-mediated cell death was reversed similarly by the mutations (Fig. 4C). These data indicate consistency among different modes of experiments with regard to reversal of potentiating effects of EFHC1 by the JME mutations but not by the coding polymorphisms. Importantly, the total amount of TRPM2 protein expression and the amount of TRPM2 protein expression in the surface membrane were indistinguishable, when TRPM2 was expressed with control GFP, wild-type or mutant GFP-EFHC1 constructs (Supplementary Fig. 3 and Supplementary Fig. 4). Furthermore, co-immunoprecipitation experiments revealed that interaction of TRPM2 with EFHC1 is unaffected by JME mutations and polymorphisms (Supplementary Fig. 5). Thus, the efficiency of JME mutations in canceling EFHC1 effects on TRPM2 function corresponds well with the previously reported reversal of neuronal death by the mutations [14].

4. Discussion

The present investigation reveals that EFHC1, the candidate gene for JME, physically interacts with the TRPM2 channel, and thereby potentiates the TRPM2 channel activity

in H_2O_2-induced cell death. The physical interaction of TRPM2 with EFHC1 is mediated by the putatively cytoplasmic TRPM2 N-terminus and C-terminus. Interestingly, the TRPM2 C-terminus contains the MutT (Nudix) motif that is the action site for TRPM2 activation triggers such as ADPR and β-NAD^+ [3–5]. Ca^{2+} channels including TRPC channels have been reported to associate with calmodulin (CaM). Considering the EF-hand-like motives present in EFHC1, EFHC1 may act as a 'Ca^{2+} sensor' like CaM, which has been reported to associate with Ca^{2+} channels including TRPC channels and to sense intracellular Ca^{2+} increment via EF-hand motives in Ca^{2+}-dependent regulation of Ca^{2+} channel activity [34–37]. We and others have previously reported that $[Ca^{2+}]_i$ is important for the TRPM2 channel activation [3,5,27,31]. Furthermore, TRPM2 activity is insensitive to CaM inhibitor, W-13, excluding the possibility that CaM participates in the regulation of TRPM2 channel activation (data not shown). Therefore, EFHC1 can indeed be the CaM-like 'Ca^{2+} sensor' responsible for Ca^{2+} dependence of activation for the TRPM2 channel. However, we found it unlikely that EFHC1 is involved in regulation of Ca^{2+} sensitivity of TRPM2 channel activation or is influenced by Ca^{2+} in TRPM2 interaction (Supplementary Fig. 2). Further studies, including examination of Ca^{2+} binding properties of EFHC1 and interaction between EFHC1 and MutT motif, are necessary to determine whether or not EFHC1 contributes to the $[Ca^{2+}]_i$-dependent regulation of TRPM2 channel activation.

We have previously suggested that EFHC1 increases the $Ca_V2.3$ Ca^{2+} current to enhance neuronal death, which may prevent unwanted hyperexcitable neurons and circuits during the development of the CNS [14]. Reduced $Ca_V2.3$ activity induced by EFHC1 mutations cannot be an exclusive mechanism that underlies JME, since mice lacking $Ca_V2.3$ gene display no seizure phenotype [38]. In this study *in situ*

hybridization analysis revealed TRPM2 and EFHC1 were coexpressed in the same cells in hippocampus and ventricles. JME mutations efficiently canceled EFHC1 effects on TRPM2 function. These results suggest that the suppression of H_2O_2-activated TRPM2-mediated Ca^{2+} influx and cell death by EFHC1 mutations contributes to expression of the JME phenotype. In fact, ROS are reported to be constitutively produced in rat hippocampus [20].

Previously, it has been demonstrated that genetic disruption of EFHC1 causes enlargement of ventricles and reduced ciliary beating frequency of ependymal cilia in the ventricle [21], and that EFHC1 interacts with microtubules to regulate cell division [22]. The reports suggest that EFHC1 and its mutations lead to the expression of JME phenotype through processes other than cell death. In this context, it is important to note that TRPM2 is co-expressed with EFHC1 in a variety of tissues including ependima, lung, and testis [5,16,17]. TRPM2 may cooperate with EFHC1 in regulation of cellular processes other than cell death in these tissues.

TRPM2 gene has been identified on human chromosome 21q22.3, where genetic disorders such as bipolar affective disorder, nonsyndromic hereditary deafness, Knobloch syndrome, and holoprosencephaly were mapped [26,39]. Furthermore, in neurons, dysregulation of redox states and intracellular Ca^{2+} homeostasis are closely implicated in the pathogenesis of neurodegenerative diseases such as Alzheimer's disease, Parkinson's disease or amyotrophic lateral sclerosis [32]. Thus, control of TRPM2 activity by EFHC1 may play an important role in the development and function of the CNS [22].

Acknowledgements

We thank T. Kajimoto for his help in drafting the manuscript and T. Takeuchi for technical assistance.

References

[1] D.E. Clapham, TRP channels as cellular sensors, Nature 426 (2003) 517–524.

[2] B. Nilius, TRP channels in disease, Biochim. Biophys. Acta. 1772 (2007) 805–812.

[3] A.L. Perraud, A. Fleig, C.A. Dunn, et al., ADP-ribose gating of the calcium-permeable LTRPC2 channel revealed by Nudix motif homology, Nature 411 (2001) 595–599.

[4] Y. Sano, K. Inamura, A. Miyake, et al., Immunocyte Ca^{2+} influx system mediated by LTRPC2, Science 293 (2001) 1327–1330.

[5] Y. Hara, M. Wakamori, M. Ishii et al., LTRPC2 Ca^{2+}-permeable channel activated by changes in redox status confers susceptibility to cell death, Mol. Cell 9 (2002) 163–173.

[6] A.L. Perraud, C.L. Takanishi, B. Shen, et al., Accumulation of free ADP-ribose from mitochondria mediates oxidative stress-induced gating of TRPM2 cation channels, J. Biol. Chem. 280 (2005) 6138–6148.

[7] E. Fonfria, I.C. Marshall, C.D. Benham, et al., TRPM2 channel opening in response to oxidative stress is dependent on activation of poly(ADP-ribose) polymerase, Br. J. Pharmacol. 143 (2004) 186–192.

[8] S. Yamamoto, S. Shimizu, S. Kiyonaka, et al., TRPM2-mediated Ca^{2+}influx induces chemokine production in monocytes that aggravates inflammatory neutrophil infiltration, Nat. Med. 14 (2008) 738–747.

[9] M. Kolisek, A. Beck, A. Fleig, R. Penner, Cyclic ADP-ribose and hydrogen peroxide synergize with ADP-ribose in the activation of TRPM2 channels, Mol. Cell 18 (2005) 61–69.

[10] K. Togashi, Y. Hara, T. Tominaga, et al., TRPM2 activation by cyclic ADP-ribose at

body temperature is involved in insulin secretion, EMBO J. 25 (2006) 1804–1815.

[11] N. Takahashi, D. Kozai, R. Kobayashi, M. Ebert, Y. Mori, Roles of TRPM2 in oxidative stress, Cell Calcium 50 (2011) 279–287.

[12] K. Uchida, K. Dezaki, B. Damdindorj, et al., Lack of TRPM2 impaired insulin secretion and glucose metabolisms in mice, Diabetes 60 (2010) 119–126.

[13] A.V. Delgado-Escueta, M.T. Mdina, J.M. Serratosa, et al., Mapping and positional cloning of common idiopathic generalized epilepsies, Adv. Neurol. 79 (1999) 351–374.

[14] T. Suzuki, A.V. Delgado-Escueta, K. Aguan, et al., Mutations in EFHC1 cause juvenile myoclonic epilepsy, Nat. Genet. 36 (2004) 842–849.

[15] C. Leon, L. de Nijs, G. Chanas, et al., Distribution of EFHC1 or myoclonin1 in mouse neural structures, Epilepsy Res. 88 (2010) 196–207.

[16] T. Ikeda, K. Ikeda, M. Enomoto, M.K. Park, M. Hirono, The mouse ortholog of EFHC1 implicated in juvenile myoclonic epilepsy is an axonemal protein widely conserved among organisms with motile cilia and flagella, FEBS Lett. 579 (2005) 819–822.

[17] T. Suzuki, I. Inoue, T. Yamagata, N. Morita, T. Furuichi, K. Yamakawa, Sequential expression of Efhc1/myoclonin1 in choroid plexus and ependymal cell cilia, Biochem. Biophys. Res. Commun. 367 (2008) 226–233.

[18] F.F. Conte, P.A. Ribeiro, R.B. Marchesini, et al., Expression profile and distribution of Efhc1 gene transcript during rodent brain development, J. Mol. Neurosci. 39 (2009) 69–77.

[19] S. Kaneko, S. Kawakami, Y. Hara, et al., A critical role of TRPM2 in neuronal cell death by hydrogen peroxide, J. Pharmacol. Sci. 101 (2006) 66–76.

[20] A.S. Driver, P.R. Kodavanti, W.R. Mundy, Age-related changes in reactive oxygen species production in rat brain homogenates, Neurotoxicol. Teratol. 22 (2000) 175–181.

[21] T. Suzuki, H. Miyamoto, T. Nakahari, et al., Efhc1 deficiency causes spontaneous myoclonus and increased seizure susceptibility, Hum. Mol. Genet. 18 (2009) 1099–1109.

[22] L. de Nijs, C. Leon, L. Nguyen, et al., EFHC1 interacts with microtubules to regulate cell division and cortical development, Nat. Neurosci. 12 (2009) 1266–1274.

[23] T. Kagawa, K. Ikenaka, Y. Inoue, et al., Glial cell degeneration and hypomyelination caused by overexpression of myelin proteolipid protein gene, Neuron 13 (1994) 427–442.

[24] S. Kiyonaka, M. Wakamori, T. Miki, et al., RIM1 confers sustained activity and neurotransmitter vesicle anchoring to presynaptic Ca^{2+} channels, Nat. Neurosci. 10 (2007) 691–701.

[25] T. Okada, S. Shimizu, M. Wakamori, et al., Molecular cloning and functional characterization of a novel receptor-activated TRP Ca^{2+} channel from mouse brain, J. Biol. Chem. 273 (1998) 10279–10287.

[26] K. Nagamine, J. Kudoh, S. Minoshima, et al., Molecular cloning of a novel putative Ca^{2+} channel protein (TRPC7) highly expressed in brain, Genomics 54 (1998) 124–131.

[27] M.E. Olah, M.F. Jackson, H. Li, et al., Ca^{2+}-dependent induction of TRPM2 currents in hippocampal neurons, J. Physiol. 587 (2009) 965-979.

[28] T. Okada, R. Inoue, K. Yamazaki, et al., Molecular and functional characterization

of a novel mouse TRP homologue TRP7: Ca^{2+} permeable cation channel that is constitutively activated and enhanced by stimulation of G-protein-coupled receptor, J. Biol. Chem. 274 (1999) 27359–27370.

[29] R. Shibata, H. Misonou, C.R. Campomanes, et al., A fundamental role for KChIPs in determining the molecular properties and trafficking of Kv4.2 potassium channels, J. Biol. Chem. 278 (2003) 36445–36454.

[30] S.F. van de Graaf, J.G. Hoenderop, D. Gkika, et al., Functional expression of the epithelial Ca^{2+} channels (TRPV5 and TRPV6) requires association of the S100A10–annexin 2 complex, EMBO J. 22 (2003) 1478–1487.

[31] D. McHugh, R. Flemming, S.Z. Xu, et al., Critical intracellular Ca^{2+}dependence of transient receptor potential melastatin 2 (TRPM2) cation channel activation, J. Biol. Chem. 278 (2003) 11002–11006.

[32] E. Bossy-Wetzel, R. Schwarzenbacher, S.A. Lipton, Molecular pathways to neurodegeneration, Nat. Med. 10 (2004) S2–S9.

[33] W. Droge, Free radicals in the physiological control of cell function, Physiol. Rev. 82 (2002) 47–95.

[34] R.D. Zuhlke, G.S. Pitt, K. Deisseroth, R.W. Tsien, H. Reuter, Calmodulin supports both inactivation and facilitation of L-type calcium channels, Nature 399 (1999) 159–162.

[35] A. Lee, S.T. Wong, D. Gallagher, et al., Ca^{2+}/calmodulin binds to and modulates P/Q-type calcium channels, Nature 399 (1999) 155–159.

[36] Y. Saimi, C. Kung, Calmodulin as anion channel subunit, Annu. Rev. Physiol. 64 (2002) 289–311.

[37] Z. Zhang, J. Tang, S. Tikunova, et al., Activation of Trp3 by inositol

1,4,5-trisphosphate receptors through displacement of inhibitory calmodulin from a common binding domain, Proc. Natl. Acad. Sci. USA 98 (2001) 3168–3173.

[38] S.M. Wilson, P.T. Toth, S.B. Oh, et al., The status of voltage-dependent calcium channels in α1E knock-out mice, J. Neurosci. 20 (2000) 8566–8571.

[39] R.E. Straub, T. Lehner, Y. Luo, et al., A possible vulnerability locus for bipolar affective disorder on chromosome 21q22.3., Nat. Genet. 8 (1994) 291–296.

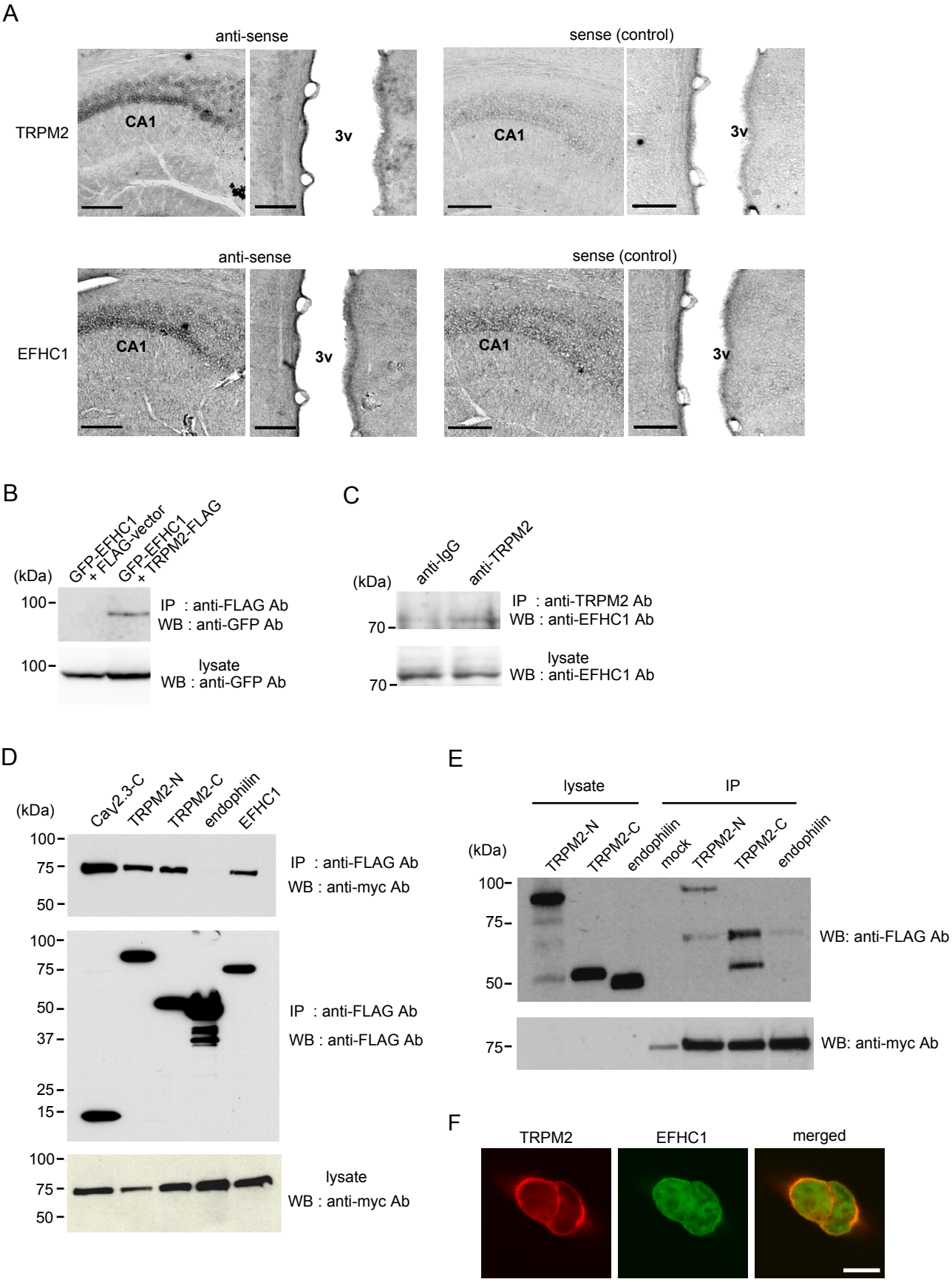
A
anti-sense
sense (control)
TRPM2
CA1
3v
EFHC1
B
(kDa)
GFP-EFHC1 + FLAG-vector
GFP-EFHC1 + TRPM2-FLAG
100
IP : anti-FLAG Ab
WB : anti-GFP Ab
lysate
WB : anti-GFP Ab
C
anti-IgG
anti-TRPM2
70
IP : anti-TRPM2 Ab
WB : anti-EFHC1 Ab
lysate
WB : anti-EFHC1 Ab
D
Cav2.3-C
TRPM2-N
TRPM2-C
endophilin
EFHC1
100
75
50
37
25
15
IP : anti-FLAG Ab
WB : anti-myc Ab
IP : anti-FLAG Ab
WB : anti-FLAG Ab
lysate
WB : anti-myc Ab
E
lysate
IP
mock
WB: anti-FLAG Ab
WB: anti-myc Ab
F
TRPM2
EFHC1
merged

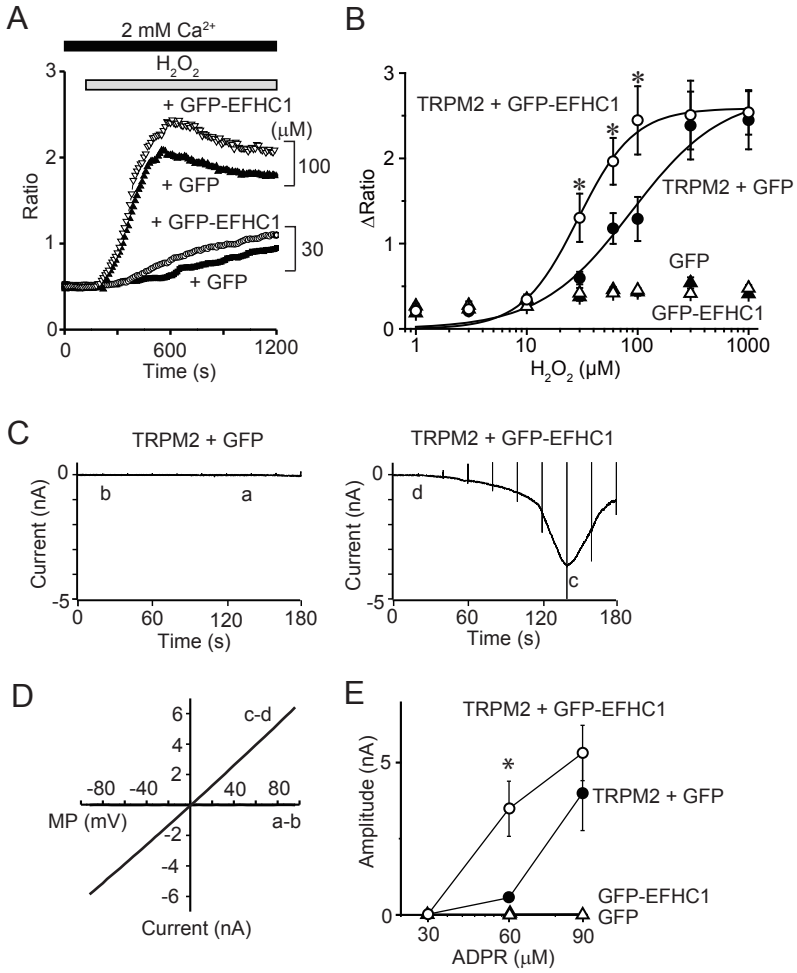
A
2 mM Ca2+
H2O2
+ GFP-EFHC1
(μM)
100
+ GFP
+ GFP-EFHC1
30
+ GFP
Ratio
Time (s)
B
TRPM2 + GFP-EFHC1
TRPM2 + GFP
GFP
GFP-EFHC1
ΔRatio
H2O2 (μM)
C
TRPM2 + GFP
TRPM2 + GFP-EFHC1
Current (nA)
Time (s)
D
c-d
MP (mV)
a-b
Current (nA)
E
TRPM2 + GFP-EFHC1
TRPM2 + GFP
GFP-EFHC1
GFP
Amplitude (nA)
ADPR (μM)

Fig. 3
Katano et al.

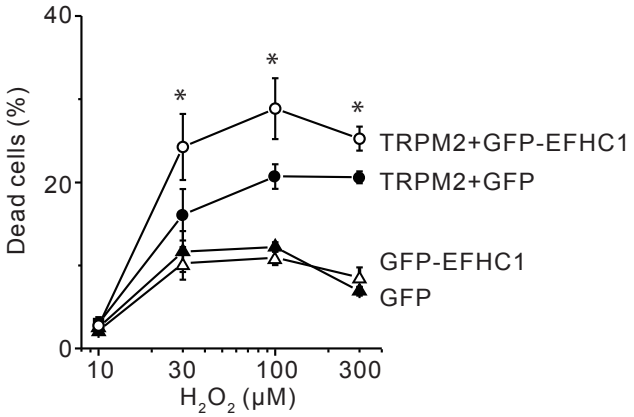

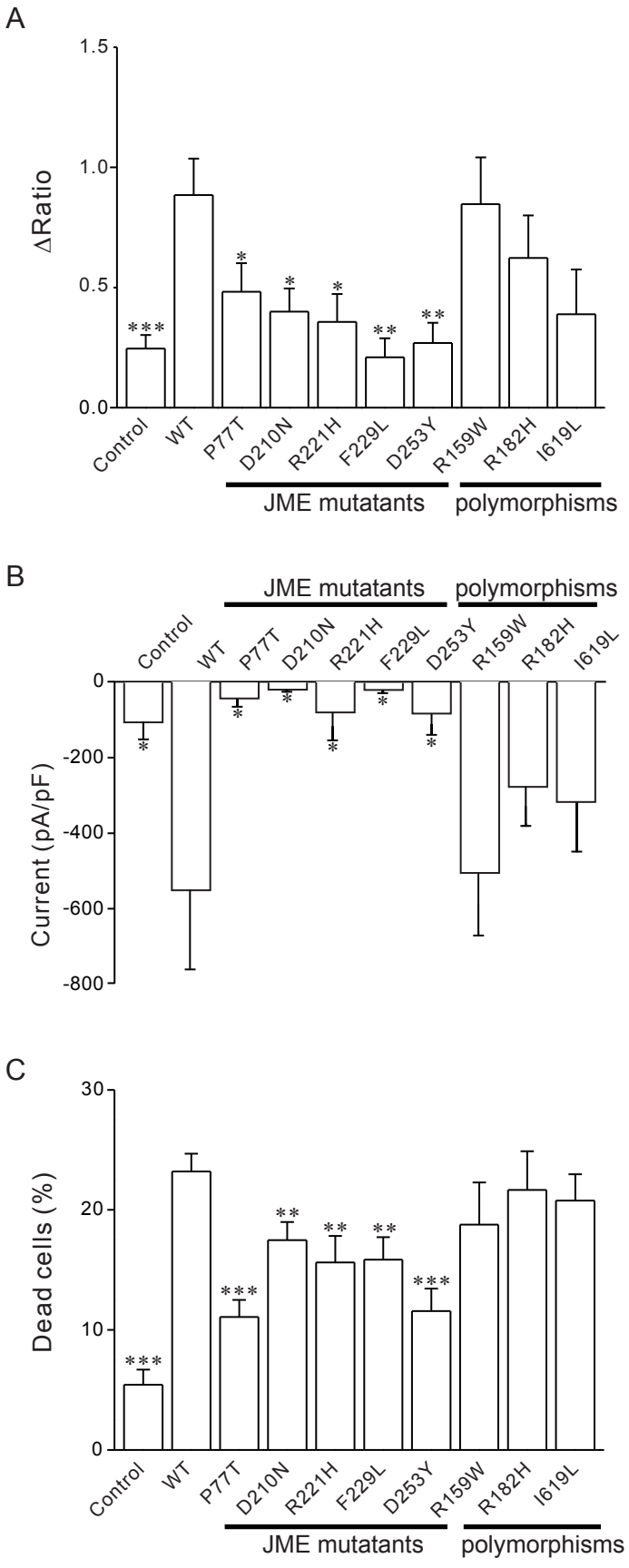
A
ΔRatio
1.5
1.0
0.5
0.0
***
*
*
*
**
**
Control
WT
P77T
D210N
R221H
F229L
D253Y
R159W
R182H
I619L
JME mutatants
polymorphisms
B
JME mutatants
polymorphisms
Control
WT
P77T
D210N
R221H
F229L
D253Y
R159W
R182H
I619L
Current (pA/pF)
0
-200
-400
-600
-800
C
Dead cells (%)
30
20
10
0
***
***
**
**
**
***
Control
WT
P77T
D210N
R221H
F229L
D253Y
R159W
R182H
I619L
JME mutatants
polymorphisms

Figure legends

Fig. 1. Direct interaction between TRPM2 and EFHC1 in HEK293 cells. A. *in situ* hybridization analysis of TRPM2 mRNA and EFHC1 mRNA in mouse brain. The transcripts of TRPM2 and EFHC1 localized at CA1 region of hippocampus and 3rd ventricle (3v). Anti-sence (left) and sense (right). Scale bar, 200 μm. B. Coimmunoprecipitation of GFP-EFHC1 with TRPM2-FLAG from HEK293 cell extracts. Immunoprecipitates (IPs) with antibody to FLAG are subjected to western blotting (WB) with antibody to GFP. C. Coimmunoprecipitation of native EFHC1 with TRPM2 from mouse brain microsome extracts. IPs with antibody to TRPM2 are subjected to WB with antibody to EFHC1. D. Identification of interaction site of TRPM2 with EFHC1. FLAG-tagged $Ca_V2.3$ C-terminus ($Ca_V2.3$-C), TRPM2 N-terminus (TRPM2-N) or C-terminus (TRPM2-C), FLAG-tagged endophilin, or FLAG-tagged EFHC1 was coexpressed with myc-tagged EFHC1 in HEK293 cells, and cell lysates were immunoprecipitated by antibody to FLAG. The $Ca_V2.3$ C-terminus or endophilin was used as positive or negative control, respectively. E. Direct interaction between TRPM2 and EFHC1 *in vitro*. FLAG-tagged TRPM2 N-terminus (TRPM2-N) or C-terminus (TRPM2-C), or FLAG-tagged endophilin was *in vitro* translated in rabbit reticulolysate. They were individually mixed with myc-EFHC1 reticulolysate, and immunoprecipitated by myc-agarose. F. Confocal images of localization of TRPM2 (red signal) and GFP-EFHC1 protein (green signal) in transiently transfected HEK293 cells. An overlay of images is shown in the right panel (yellow signal). Scale bar, 10 μm.

Fig. 2. Potentiation of H_2O_2-induced TRPM2 activation by EFHC1. A. Potentiation of H_2O_2-induced $[Ca^{2+}]_i$ rises detected in TRPM2 and EFHC1-coexpressing HEK293 cells.

B. Mean responses for maximum ratio rises (ΔRatio) induced by H_2O_2 in HEK293 cells transfected with TRPM2 and EFHC1. TRPM2 and GFP-EFHC1 (open circles), TRPM2 and GFP (closed circles), GFP-EFHC1 (open triangles), GFP (closed triangles). H_2O_2 concentration-response plots were fitted to the Hill equation: $r = b + (a-b) C^n/(e^n+C^n)$, where *r* is the response, a is the maximum response, b is the basal response, C is the H_2O_2 concentration (in μM), e is the EC_{50}, and *n* is Hill coefficient. HEK293 cells expressing TRPM2 and GFP-EFHC1; EC_{50}: 29 ± 3.3 μM; Hill coefficient: 1.7, HEK293 cells expressing TRPM2 and GFP; EC_{50}: 88 ± 29 μM; Hill coefficient: 1.1. C. Electrophysiological analysis of TRPM2 channel coexpressed with EFHC1. Representative traces of the currents of TRPM2 channels coexpressed with GFP (left panel) or GFP-EFHC1 (right panel) in response to 100 μM ADPR. Holding potential was –60 mV. Fifty-ms triangular voltage ramps from –100 mV to 100 mV were applied every 20 s. D. Current-voltage (*I-V*) relationships of the ADPR-induced TRPM2 current. *I-V* relationships were obtained by subtracting currents before activation of channels from those after activation (indicated by small letters in C). MP indicates membrane potential. E, Mean responses for maximum amplitude induced by ADPR. Data points are the means ± S.E.. *, $P<0.05$, compared with TRPM2 and GFP-coexpressing HEK293 cells.

Fig. 3. Potentiation of TRPM2-dependent cell death by EFHC1. Viability assessed by trypan blue exclusion. Cells coexpressed with TRPM2 and GFP or GEP-EFHC1 were exposed to various concentration of H_2O_2 in HBS solution for 20 min. Data points are the means ± S.E.. *, $P<0.05$, compared with TRPM2 and GFP-coexpressing HEK293 cells.

Fig. 4. Reversal of EFHC1-induced enhancements of TRPM2 activity and cell death by JME mutations. A. ΔRatio induced by H_2O_2 in HEK293 cells coexpressing TRPM2 with GFP (Control), EFHC1 (WT) or GFP-EFHC1 mutants. The cells were stimulated with 30 μM H_2O_2. B. Maximum current density induced by 100 μM ADPR in HEK293 cells coexpressing TRPM2 with GFP (Control), EFHC1 (WT) or GFP-EFHC1 mutants. Fifty-ms triangular voltage ramps from –100 mV to 100 mV were applied every 10 s from a holding potential of 0 mV. C. Potentiation of TRPM2-dependent cell death by EFHC1 and its reversal by JME mutations. Cell death is assessed by trypan blue exclusion among GFP positive cells. Cells coexpressing TRPM2 with GFP (Control), GFP-EFHC1 (WT) or GFP-EFHC1 mutants were exposed to 30 μM H_2O_2 in HBS solution for 20 min. Data points are the means ± S.E.. *, ** and *** indicate $P<0.05$, $P<0.01$ and $P<0.001$, respectively, compared with cells coexpressing TRPM2 and GFP-EFHC1 (WT).

Supplementary Fig. 1
Katano et al.

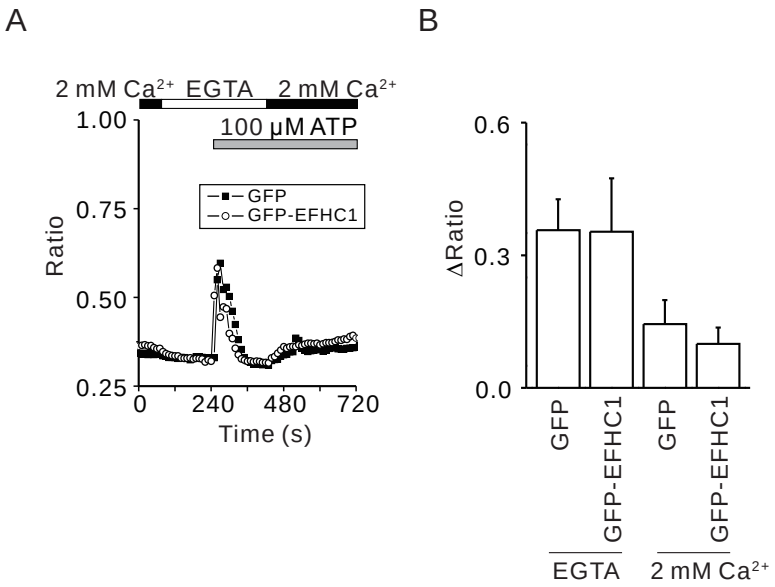

Supplementary Fig. 1. Effect of EFHC1 protein on Ca^{2+} release activity from intracellular Ca^{2+} stores in response to 100 μM ATP. A. ATP-induced Ca^{2+} rises were measured in GFP or GFP-EFHC1-expressed HEK293 cells in the absence of extracellular Ca^{2+} (EGTA). B. Mean responses for maximum ratio rises (ΔRatio) induced by 100 μM ATP. Data points are the means ± S.E..

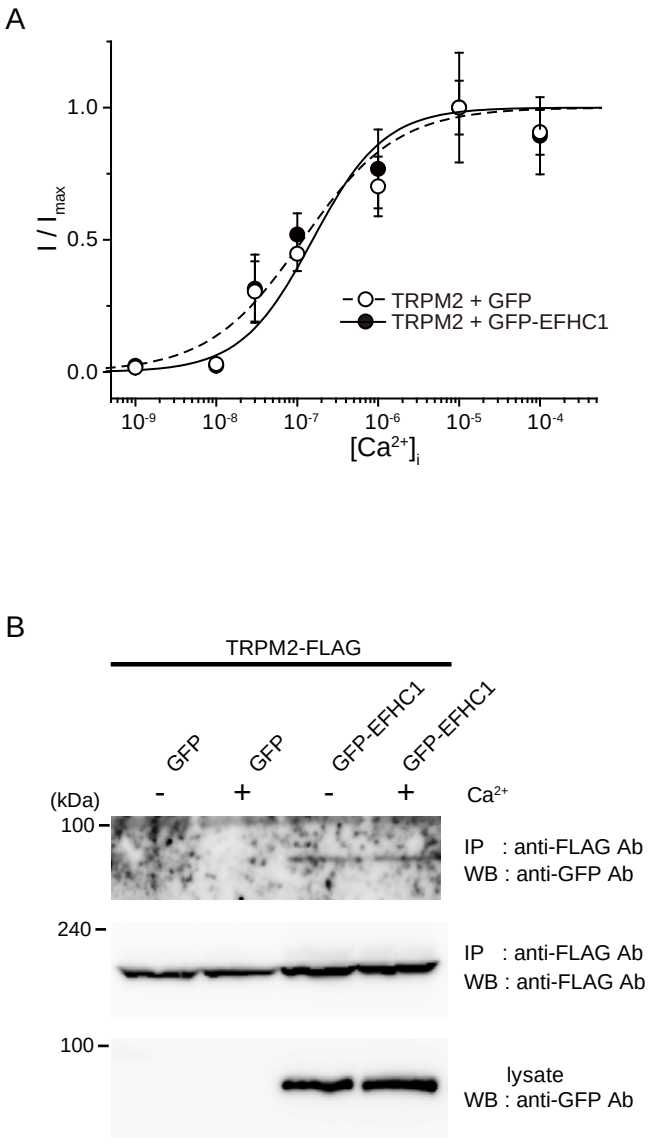

Supplementary Fig. 2. Effects of intracellular Ca^{2+} concentration on TRPM2 activity and physical interaction of TRPM2 with EFHC1. A. TRPM2 whole cell currents were obtained in response to 100 μM ADPR at –100 mV in HEK293 cells coexpressing with GFP (open circle) or GFP-EFHC1 (closed circle). Holding potential was 0 mV. Fifty-ms triangular voltage ramps from –100 mV to 100 mV were applied every 10 s. The peak amplitudes are normalized to those at $[Ca^{2+}]_i$ of 10 μM. Data are the means ± S.E.. Concentration response plots were fitted to the Hill equation (see Experimental procedure 2-7). For TRPM2 + GFP, EC_{50} is 117 ± 35 μM and Hill coefficient is 0.7. For TRPM2 + GFP-EFHC1, EC_{50} is 155 ± 70 μM and Hill coefficient is 1.0. B. Effects of Ca^{2+} concentration on physical interaction of TRPM2 with EFHC1 by immunoprecipitational analysis. FLAG-tagged TRPM2 C-terminus (TRPM2-FLAG) was coexpressed with GFP or GFP-tagged EFHC1 in HEK293 cells, and the cell lysates were immunoprecipitated by antibody to FLAG in the presence or absence of 100 μM Ca^{2+}.

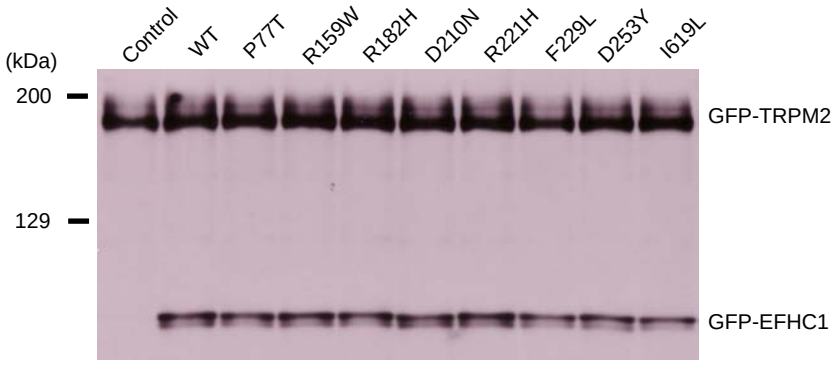

Supplementary Fig. 3. Detection of TRPM2 and EFHC1 proteins in transiently transfected HEK293 cells. GFP-TRPM2 and GFP (Control), GFP-EFHC1 (WT) or EFHC1 mutant proteins were detected by western blot analysis using an anti-GFP antibody.

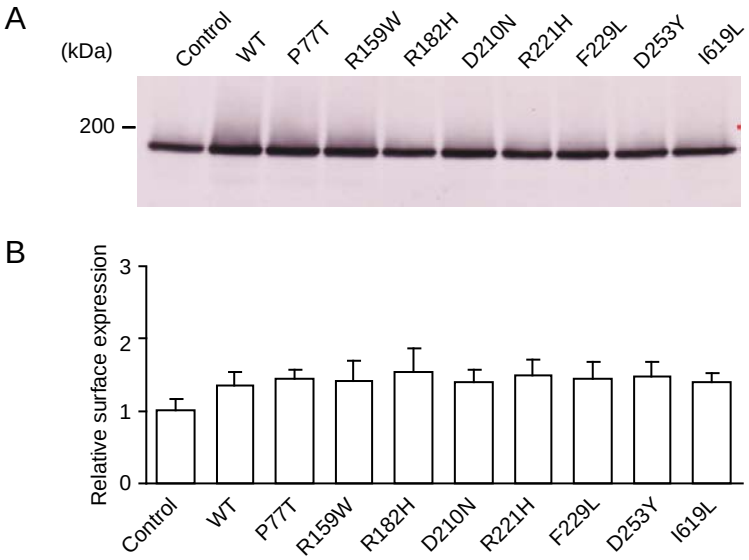

Supplementary Fig. 4. Cell surface expression of GFP-TRPM2. HEK293 cells are cotransfected with GFP-TRPM2 and GFP (Control), GFP-EFHC1(WT), or EFHC1 mutants. The cell lysate prepared after exposure to NHS-SS-biotin is incubated with streptavidin-agarose, and the obtained surface proteins are analyzed by WB. A. WB with anti-GFP antibody. B. Relative surface expression compared with control. Surface expression is statistically indistinguishable among HEK293 cells cotransfected with GFP-TRPM2 and Control, WT, or EFHC1 mutants.

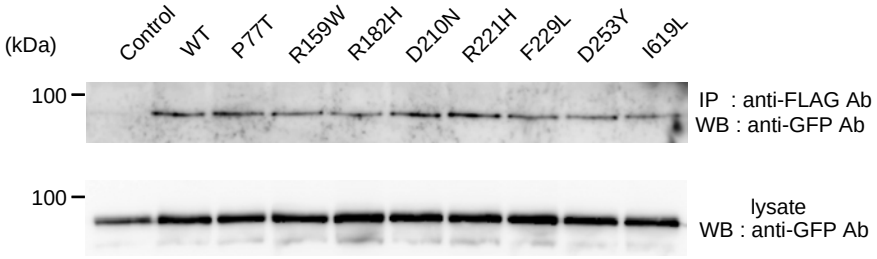

Supplementary Fig. 5. Coimmunoprecipitation of GFP-EFHC1 (WT) or the mutants with TRPM2-FLAG from HEK293 cell extracts. Immunoprecipitates with antibody to FLAG are subjected to WB with antibody to GFP.

Supplemental methods

Biotinylation of cell surface proteins

HEK293 cells were coexpressed with GFP-tagged TRPM2 and GFP, GFP-tagged EFHC1 or GFP-tagged EFHC1 mutants. The cells were washed twice with ice-cold PBS and then incubated for 30 min at 4°C with 2 mg/ml Sulfo-NHS-SS-Biotin (Pierce). The biotinylation reaction was terminated by washing the cells 3 times with ice-cold PBS containing 10 mM glycine. The cells were then lysed with 300 μl of ice-cold RIPA buffer for 30 min at 4°C. The cell extracts were cleared by centrifugation and added to 100 μl of streptavidin-agarose beads (Pierce) (50% slurry, pre-equilibrated in RIPA buffer) and incubated for 16 h at 4°C. The biotin-streptavidin-agarose complexes were harvested by centrifugation and washed five times with RIPA buffer. The beads were then resuspended in 2 × sample buffer and incubated at room temperature for 30 min before SDS-PAGE fractionation and Western blotting.